



EPIC Geolocation and Color Imagery Algorithm Revision 6

October 10, 2019



**National Aeronautics and
Space Administration**

Karin Blank
NASA/GSFC
Code 586

**Goddard Space Flight Center
Greenbelt, Maryland**



Distributed by the Atmospheric Science Data Center
<http://eosweb.larc.nasa.gov>



1	Overview	5
1.1	Instrument Characteristics.....	5
1.2	Objectives of L1A/L1B geolocation	6
1.3	Retrieval Strategy	6
2	Algorithm Description	7
2.1	Algorithm Input (EPIC & Non-EPIC)	7
2.2	Theoretical Description of Geolocation	7
2.2.1	3D Model Generation.....	7
2.2.2	Image Registration	7
2.2.3	3D Model to 2D Image Plane Conversion	8
2.2.4	L1A Description.....	8
2.2.5	L1B Description	9
3	Mathematical Description of Algorithm	11
3.1	Image Registration	11
3.1.1	Mask Generation	11
3.1.2	Masking algorithm	12
3.1.3	Centering – Coarse Alignment.....	13
3.2	Spacecraft Orientation.....	13
3.2.1	Ephemerides Interpolation	14
3.2.2	Quaternion Interpolation	14
3.2.3	Attitude Determination.....	15
3.3	Astronomical Model.....	16
3.3.1	Right Ascension and Declination.....	17
3.3.2	Mean Sidereal Time	17
3.3.3	Julian Dynamical Time	18
3.3.4	Nutation.....	18
3.3.5	True Obliquity	19
3.3.6	Apparent Sidereal time.....	20
3.3.7	Precession.....	20
3.3.8	Apparent Right Ascension and Declination	21
3.3.9	Parallax.....	21
3.3.10	Azimuth and Elevation.....	22
3.4	2D Transform	22
3.4.1	EPIC Azimuthal Projection.....	22
3.4.2	Atmospheric Refraction	24
3.4.3	Area Mapping.....	25
3.4.4	Optical Correction	26
3.4.5	Subpixel Correction.....	27
3.5	Correction for attitude error	28
3.6	Level 1A Algorithm	28
3.7	Level 1B Algorithm	29
3.7.1	Multi-day alignment.....	29
4	Color Imagery.....	31
4.1	Rayleigh scattering.....	32
4.2	CIE Color System.....	34



5	Algorithm Output.....	37
5.1	Level 1A.....	37
5.1.1	Band Group	37
5.2	Level 1B.....	39
5.3	Geolocation metadata.....	42
6	Appendix	45
6.1	Periodic terms for calculation of nutation.....	45
6.2	Rayleigh correction factor.....	45
7	Revision updates.....	48
7.1	Updates from Revision 4 to 5.....	48
7.2	Updates from Revision 5 to 6.....	48
8	References	48



ACKNOWLEDGEMENTS

Many thanks to:

Liang-Kang Huang, who spent significant time testing and validating the products, and for solving the focal length question.

Semion Kizhner, for writing the code to implement the atmospheric refraction correction.

Rick Coon, for providing assistance with the calculations for attitude.

Jay Herman, Adam Szabo, Sasha Marshak, and the level 2 science teams for their patience in waiting for the quirks to be resolved.



1 OVERVIEW

The Deep Space Climate Observatory (DSCOVR) is a joint National Oceanic and Atmospheric Administration (NOAA) and National Aeronautics and Space Administration (NASA) mission. NOAA is responsible for day-to-day operations of the spacecraft, Earth science and space weather instruments, while NASA provides the science expertise and processing for the Earth science instruments. DSCOVR was launched February 11th, 2016 and orbits the Earth-Sun Lagrange point (L1).

This document concerns the geolocation algorithms used for the Earth Polychromatic Imaging Camera (EPIC). For more information regarding the DSCOVR mission and EPIC technical specifications please refer to the “Deep Space Climate Observatory Earth Science Instrument Overview” document. A brief description of EPIC is offered in the section below.

1.1 INSTRUMENT CHARACTERISTICS

EPIC is a Cassegrain telescope using a Charge Coupled Device (CCD) detector. It samples narrow bands in the ultraviolet, visible, and infrared covering a range of 317-780nm. Using these bands, it is possible to measure ozone, aerosols, cloud reflectivity, cloud height, and vegetation properties. Two filter wheels are used to image the different spectral bands.

The basic specifications concerning the instrument are as follows.

CCD:

Model	Fairchild Imaging 442A
Resolution	2048 x 2048 pixels
Pixel size	15um x 15um
Imaging area	30.72mm x 30.72mm
Bit depth	12 bits

Telescope:

Aperture	30.5
Focal length	283.82 cm
Field of view	.61 degrees

Filter Wheel:

Band Name	Wavelength (nm)	Full Width (nm)	Band Type
317nm	317.5 ± .1	1 ± .2	Ultraviolet
325nm	325 ± .1	2 ± .2	Ultraviolet
340nm	340 ± .3	3 ± .6	Ultraviolet
388nm	388 ± .3	3 ± .6	Ultraviolet
443nm	443 ± 1	3 ± .6	Visible
551nm	551 ± .1	3 ± .6	Visible
680nm	680 ± .2	2 ± .4	Visible



688nm	$687.75 \pm .2$	$.8 \pm .2$	Visible
764nm	$764 \pm .2$	$1 \pm .2$	Infrared
780nm	$779.5 \pm .3$	$2 \pm .4$	Infrared

1.2 OBJECTIVES OF L1A/L1B GEOLOCATION

The objective of L1A/B geolocation is to provide ancillary information regarding the EPIC images that require instrument and spacecraft specific knowledge. This includes per pixel latitude and longitude locations, as well as sun and instrument viewing angles. All metadata used to calculate these solutions is as well included, including spacecraft and body ephemerides, attitude, and any other ancillary information.

In the L1A this information is appended; in L1B it is applied. For L1A this means that the images are in their natural coordinates as originally taken by the spacecraft. Geolocation is oriented to match the original image and location and angle information is available on a per-image basis.

For L1B, the images are corrected such that their orientation is the same across the entire 10 band set. This means that the images are rotated so North is aligned with the top, as well as corrected for the Earth's rotation on its axis. For the appended location data, latitude and longitude is the same for all 10 bands, however the sun angles are different for each band.

1.3 RETRIEVAL STRATEGY

There are a number of challenges in solving the problem of EPIC geolocation. The first is that the DSCOV star tracker accuracy is not sufficient enough to resolve pointing to the pixel level. This requires measurements be made on the images themselves to derive pointing corrections.

The second is that as EPIC rotates through the filter wheels, taking the 10 images that comprise a set, the Earth is also rotating. In the time that it takes to complete a nominal set, about 7 minutes, there is a non-linear 4-pixel drift between the first image and the last. To solve this requires the ability to build dynamic transformation calculations that can handle not only variances in the image timing, but also non-nominal imaging scenarios, such as custom cadences.

The third is that the view EPIC has of the Earth possess unique challenges that are not typical of conventional Earth science instruments. Some of these are related to the fact that there can be no "flat earth" approximations to any calculations – the full body of the Earth must be rendered accurately. Others relate to issues with the wide spatial view that are typically minimal in other missions, such as distortion from atmospheric refraction.



2 ALGORITHM DESCRIPTION

In the following sections are two descriptions of the algorithm. The first is a high-level overview of how the algorithm operates. The second is the mathematical description of the algorithm.

2.1 ALGORITHM INPUT (EPIC & NON-EPIC)

The input for the algorithm from EPIC is the calibrated L1A images, the original L0 images; sun, lunar, and spacecraft ephemerides, attitude information, and the EGM2008 terrain information.

The calibrated L1A images are used for the image processing and are ultimately what are put in the L1A product; the L0 images are used to obtain metadata from the headers.

Sun, lunar, and spacecraft ephemerides, as well as attitude information, provide information on how the Earth or other bodies is oriented in the field of view. The EGM2008 terrain datasets is used for modeling Earth's body.

2.2 THEORETICAL DESCRIPTION OF GEOLOCATION

This section contains a high-level overview of geolocation. A detailed mathematical description follows in section 3. At the top level, there are three main parts of the system. There is the first part that takes the ancillary information regarding the scene and builds a 3D model of the Earth as seen at the time the image was taken. The second part is the image registration algorithm that registers the images to the 3D model. The final part redraws the 3D model into the 2D plane.

2.2.1 3D Model Generation

The 3D model is built using the ancillary information from the spacecraft. This includes the sun, lunar, and spacecraft ephemerides with Earth as the coordinate reference frame (J2000), the spacecraft attitude information, and the time the image was taken. Using this information and relative astronomical algorithms, it builds a complete 3D model of the scene, in geodetic coordinates, as well as the viewing and solar angles. Using the complete surface viewing angles, it determines the orientation of the Earth in regard to the spacecraft at the time and derives the ancillary information necessary to convert this information to the 2D plane, where it provides per-pixel ancillary data mapped to the original EPIC image.

2.2.2 Image Registration

For image registration, the 2D XY correction to center the Earth in the image is calculated. For EPIC, it is not possible to determine the correction using the DSCOVER star tracker information alone, as its accuracy is only sufficient enough to guarantee the Earth remains in EPIC's field of view. Therefore it is necessary to derive the XY image offset of Earth's center by using data derived from the image.

In order to do this, a mask of the Earth pixels is generated. A coarse estimate is initially derived by calculating the X and Y chord lengths of the object in the image. The



longest chords, which represent the location of the object's center, are then used to derive the coarse X and Y offset.

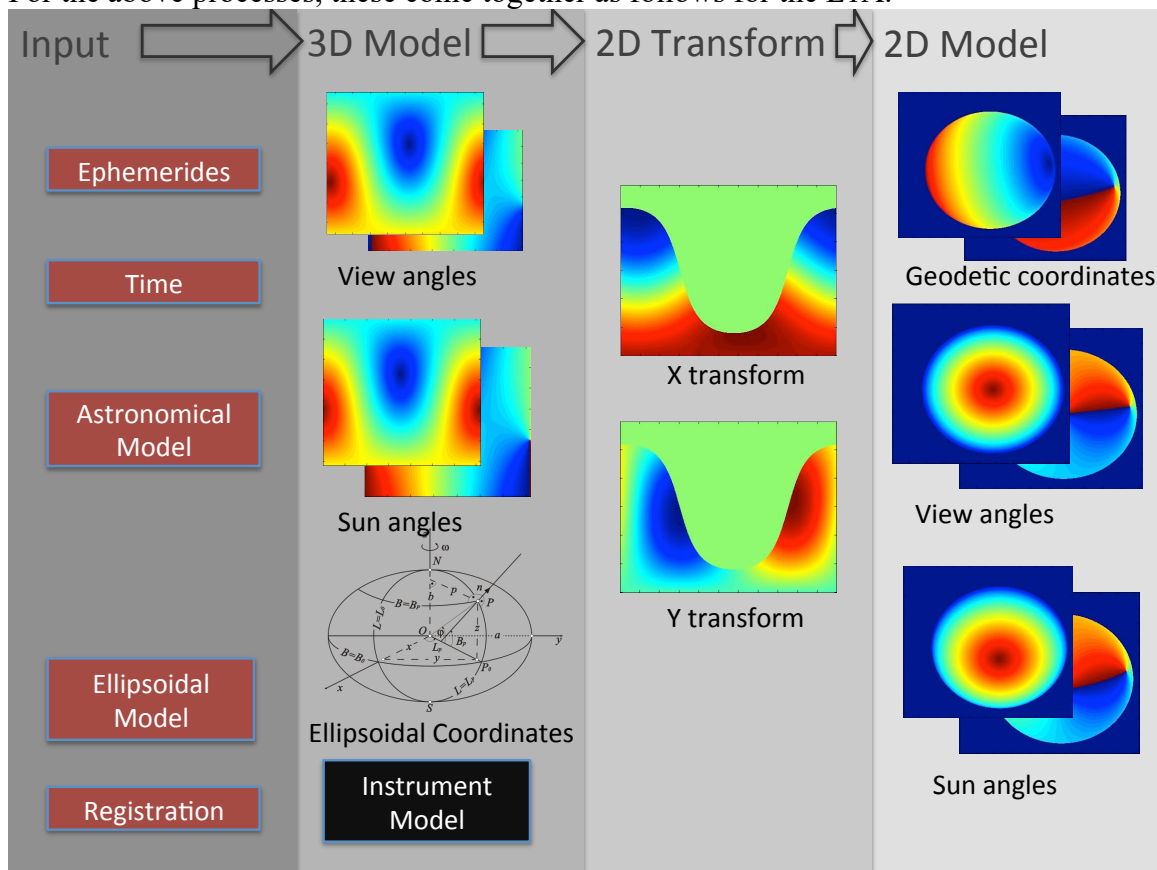
2.2.3 3D Model to 2D Image Plane Conversion

The process of the image registration permits the data to be registered to the 3D Earth model. Every pixel is mapped to a corresponding geodetic coordinate – latitude, longitude and surface height, as well as sun/spacecraft azimuth and elevation angles. It is important to note that the 3D model is complete – it contains information regarding the non-viewable surfaces as well. This makes it possible to do transformations without regard to surface boundary conditions, as there is a complete mathematical solution for every point.

To perform the 3D to 2D conversion, the 3D model is mapped into the “EPIC plane” which is a projection based on EPIC's physical and optical parameters. To do this, the transformation is passed the 3D model and desired nadir point. A transformation is constructed that maps the 3D coordinates to 2D image coordinates and the 3D data is redrawn in the 2D EPIC plane. In the case of L1A, the ancillary data is redrawn with the relative X, Y, and rotational offsets to match the original image. For L1B, ancillary data and image are redrawn to the set reference frame.

2.2.4 L1A Description

For the above processes, these come together as follows for the L1A.



Input - The algorithm accepts the sun, spacecraft, and lunar ephemerides, time, and attitude. The astronomical and ellipsoidal models are predefined algorithms. An image registration algorithm is used to derive X and Y offsets for the Earth.

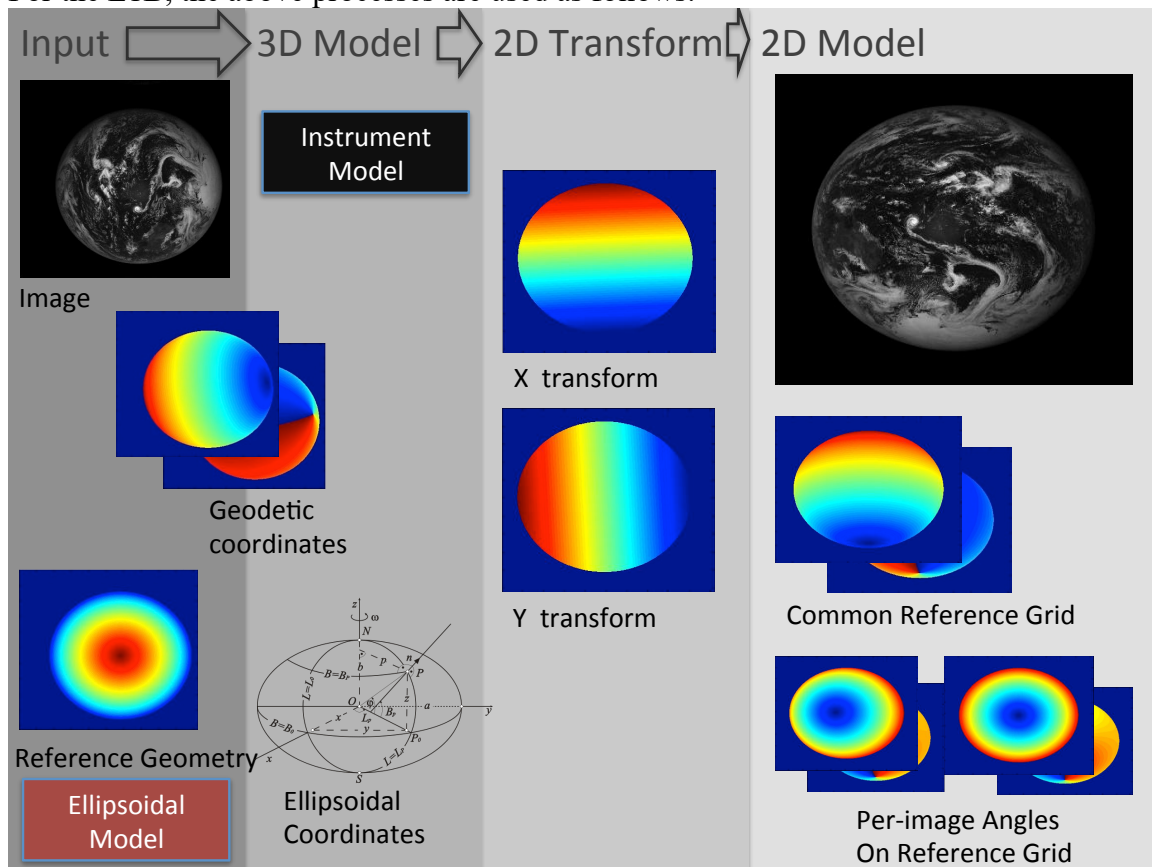
3D Model - The 3D model algorithm is then run to generate the latitude, longitude, sun and spacecraft angles for the full globe.

2D Transform - The 2D transformation is run against the 3D model to generate per-pixel latitude, longitude, sun and spacecraft angles to match the calibrated L1A image in its original orientation. Optical distortion seen in the EPIC lens is applied as part of this process.

2D Model - The transformation generates the data in the EPIC projection. This includes 2D geolocation information, which consists of latitude, longitude, sun zenith angles, sun azimuth, spacecraft zenith angles, and spacecraft zenith angles.

2.2.5 L1B Description

For the L1B, the above processes are used as follows.



Input - The image, latitude, longitude datasets, as well as viewing metadata read from the L1A file. This is used to fill the 3D model.

3D Model - The next step is to select a common reference frame. This will provide the reference geometry for the 3D to 2D transformation. It selects the image taken in the middle of the sequence, as this will provide the most uniform results for all images with the rotation.



2D Transform - Sun and spacecraft angles are generated for each image based on the reference geometry and the time the particular image was taken.

2D Model - The original L1A image, which is now part of the 3D model, is rendered using the 3D to 2D transformation, and is redrawn in the 2D EPIC imaging plane. EPIC's optical distortion is removed during this process. This produces the L1B image.

The georeferenced L1B image, latitude, longitudes, and sun and spacecraft viewing angles are written to the L1B file.



3 MATHEMATICAL DESCRIPTION OF ALGORITHM

The following is the mathematical description of the geolocation algorithm. This contains the algorithmic details of the higher-level description in section 2.2.

3.1 **IMAGE REGISTRATION**

In order to align Earth with its geophysical model, it is necessary to compute its X, Y location of the planetary body's center in relation to the image. This compensates for the pointing offsets inherent to DSCOVER's attitude control. The accuracy needs to be at the subpixel level. To accomplish this, all registration is done on a bicubic-interpolated version of the image, which has been enlarged to 4x resolution.

Figure 1 is an example of the before and after of the registration process. Note that the before image is an atypical case used for illustration purposes ; nominal performance of DSCOVER's pointing has better accuracy.

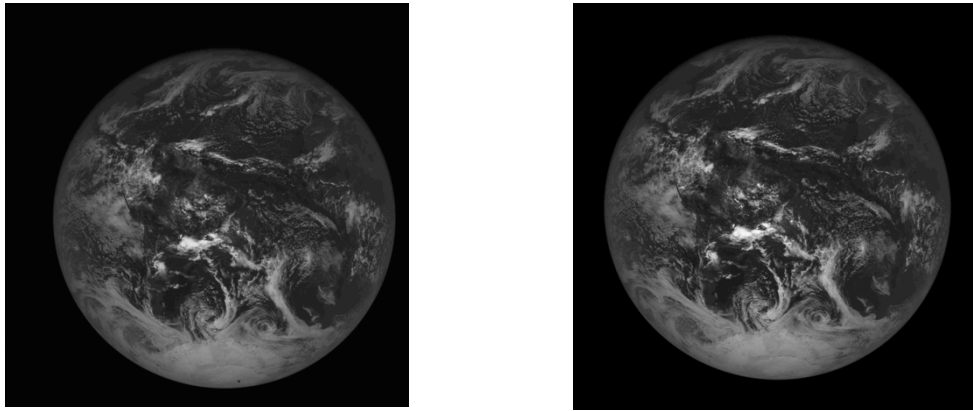


Figure 1 - Image on left is before centering. Image on right is after centering

3.1.1 Mask Generation

The first element of the registration is to build a mask of Earth pixels in the image. In the mask, ones are Earth pixels, and zeros are dark space. The masking algorithm uses several common morphological algorithms defined as below.

Erosion is a morphological operator that removes poorly connected pixels. It is used to remove stray noise pixels and smooth edges.

Erosion of image A by binary structure element B is defined as:

$$A \ominus B = \{z | (B)_z \subseteq A\}$$

Dilation is a morphological operator that improves connectivity between common pixels. It is used to fill holes and smooth edges.

Dilation of image A by binary structure element B is defined as:



$$A \oplus B = \{z | [(\hat{B})_z \cap A] \subseteq A\}$$

Opening is a morphological operator that smooths contours of an object, eliminating small indents and protrusions. It is built of both erosion and dilation operators.

Opening of set A by structure element B is defined as:

$$A \circ B = (A \ominus B) \oplus B$$

Closing is a morphological operator that removes small objects and edge noise from an object.

Closing of set A by structure element B is defined as:

$$A \cdot B = (A \oplus B) \ominus B$$

A region-filling operator sets small, zero valued pixels to 1 if they are within a bounded object.

Region filling is defined as, for a set of binary elements X and B is a structuring element, the procedure to fill bounded regions by one is:

$$X_k = (X_{k-1} \oplus B) \cap A^c \quad k = 1, 2, 3 \dots$$

A connectivity operator searches for connected pixels. It returns the indexed groups of connected pixels. This operator is used to remove any large object noise or optical artifacts from the mask.

The following iterative expression searches through an image, returning sets of connected components, Y.

$$Y = (X_{k-1} \oplus B) \cap A \quad k = 1, 2, 3 \dots$$

3.1.2 Masking algorithm

The above algorithms are put together to define the EPIC masking algorithm. This algorithm thresholds the image against known dark count levels and removes noise and instrument artifacts from the mask.

For the following equations, a binary image A_0 is constructed by thresholding an EPIC image against a known factor. For the morphological operators, B_x are square structuring elements of size x .

The first step is to remove weak noise and connectors from the image via:

$$A_1 = A_0 \cdot B_5$$



And then to strengthen remaining connections and edges via:

$$A_2 = A_1 \circ B_5$$

Objects with closed boundaries are then filled:

$$X_k = (X_{k-1} \oplus B) \cap A_2^c \quad k = 1, 2, 3 \dots$$

And then indexed by connectivity:

$$Y = (X_{k-1} \oplus B_4) \cap A \quad k = 1, 2, 3 \dots$$

The largest object is then retained and edges are smoothed and filled:

$$A_3 = Y_{max} \cdot B_{40}$$

The masked data set generated is then used for the coarse alignment. Figure 2 demonstrates the results of the masking algorithm using the image example in Figure 1.

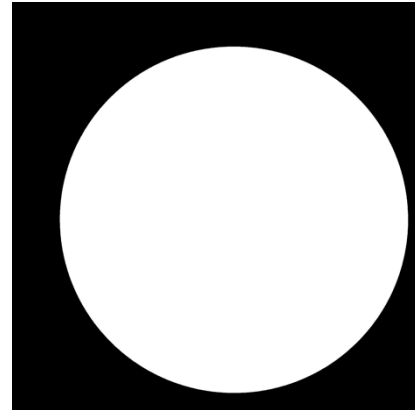


Figure 2 - Example of generated mask

3.1.3 Centering – Coarse Alignment

The first attempt in obtaining the XY centering values is to do a coarse alignment on the image mask. On a gridded surface such as an image, it is only possible to navigate straight lines at 45-degree angles. The coarse alignment measures the chords of the Earth's masks at these angles and uses it to estimate the XY offset required to center the Earth.

3.2 SPACECRAFT ORIENTATION

Determining the spacecraft's orientation is necessary for determining what EPIC is pointed at and the related angles. DSCOVR is not stationary at the Earth-Sun Lagrange; instead it orbits in a Lissajous figure over a time period of 6 months. The spacecraft additionally rolls during the orbit and has no fixed orientation in regard to Earth's reference frame. EPIC is also not always Earth pointing; there are times when it takes images of other objects, such as the Moon, for calibration purposes, or where there are off-pointing

Lissajous Orbit Viewed from Earth

(15°, 15°, 4°) Class 2/CCW, 5 years
6 month period for a single loop

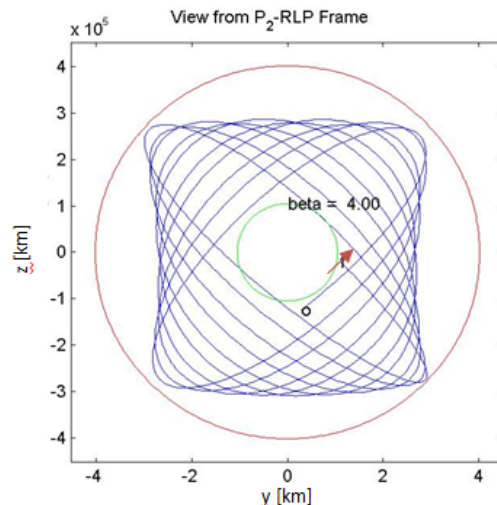


Figure 3 - Example of Lissajous orbit



activities into deep space to calibrate the other instruments on-board.

The desired outputs of these calculations are the determination what EPIC is currently viewing, either Earth, Moon, or dark space, and the roll angle for Earth's North pole. The inputs to the calculations are the sun and spacecraft ephemerides, attitude, image time, and Earth's X, Y image coordinate offsets.

The first step is to determine the spacecraft's positioning.

3.2.1 Ephemerides Interpolation

The DSCOVR ephemerides are produced at 1-minute intervals. These are in the J2000 coordinate reference frame. To calculate the ephemerides at a specific time interval, interpolation uses a piecewise hermite spline to generate X, Y, and Z coordinates.

3.2.2 Quaternion Interpolation

DSCOVR attitude information is generated at 30 second to 10 second intervals from the star tracker, with occasionally longer gaps due to missing telemetry. The star tracker is accurate enough to determine general pointing information, such as what body is being imaged, but does not produce a tilt and yaw angle accurate enough for geolocation. However, as the spacecraft orbits L1 it slowly rotates with respect to Earth – the exact rate is dependent on the location in orbit. This roll angle is required in order to orient the images with north up.

Quaternion interpolation requires using a device known as SLERP – Spherical Linear Interpolation. With SLERP, interpolations are done along a sphere, as opposed to a line, permitting smooth quaternion generation through rotations.

The calculation of SLERP is as follows.

For where t_a and t_b are the first and second time interval, q_a and q_b are their corresponding quaternions, and t_m is the time interval to interpolate to:

$$t = \frac{t_m - t_a}{t_b - t_a}$$

The half angle between q_a and q_b is then:

$$\frac{\theta_{ab}}{2} = \cos^{-1}(q_{a4} * q_{b4} + q_{a1} * q_{b1} + q_{a2} * q_{b2} + q_{a3} * q_{b3})$$

The ratio between the angles is then:

$$r_a = \frac{\sin(1 - t) \frac{\theta_{ab}}{2}}{\sqrt{(1 - \frac{\theta_{ab}^2}{2})}}$$



$$r_b = \frac{\sin(t - \frac{\theta_{ab}}{2})}{\sqrt{(1 - \frac{\theta_{ab}^2}{2})}}$$

And the interpolated quaternion is then:

$$q_m = q_a r_a + q_b r_b$$

3.2.3 Attitude Determination

Attitude determination is used to generate a coarse pointing estimate and the image rotational correction.

It is worth noting that in the Triana AOCS Hardware Coordinate System Document, there are a series of coordinate transformation that were applied to go from the spacecraft body to the EPIC reference frame. These are not necessary for any dates after June 19th, 2015, a few days after “first light” for EPIC. This is because the star tracker for DSOCVR was calibrated and aligned to EPIC, making EPIC the reference frame for the spacecraft.

To determine the spacecraft orientation in Euler coordinates, it is necessary to do two steps. The first is to interpolate the quaternions to the current time. The second is to convert quaternions to a cosine attitude matrix, and apply the appropriate transformations, which include corrections for precession and nutation. The final step is to convert the cosine attitude matrix to Euler coordinates, which provides angles in the image reference frame.

A quaternion, q , can be converted to a cosine attitude matrix, A , via:

$$A_q = \begin{bmatrix} q_1^2 - q_2^2 - q_3^2 + q_4^2 & 2(q_1 q_2 + q_3 q_4) & 2(q_1 q_3 - q_2 q_4) \\ 2(q_1 q_2 - q_3 q_4) & -q_1^2 + q_2^2 - q_3^2 + q_4^2 & 2(q_2 q_3 + q_1 q_4) \\ 2(q_1 q_3 + q_2 q_4) & 2(q_2 q_3 - q_1 q_4) & -q_1^2 - q_2^2 + q_3^2 + q_4^2 \end{bmatrix}$$

Conversion to Earth Centered Rotational Coordinates requires using the apparent sidereal time (asrt) from section 3.3.

$$A_{asrt} = \begin{bmatrix} \cos(asrt) & \sin(asrt) & 0 \\ \sin(asrt) & -\cos(asrt) & 0 \\ 0 & 0 & 1 \end{bmatrix}$$

The Earth Centered Rotational coordinates are then:

$$A_{ECR} = A_{asrt} A_q$$

Conversion from Cosine Attitude Matrix to Euler coordinates requires knowing the spacecraft rotation sequence – DSCVR is 3-2-1 (ZYX).



To obtain the spacecraft roll (ϕ):

$$\phi = \tan^{-1} \frac{A_{12}}{A_{11}}$$

To determine what EPIC is pointed at requires calculating the pointing vector. In the following, sc is the spacecraft ephemeris coordinates, and sun is the sun vector. This calculates the pointing vector between the spacecraft and Earth. To calculate the pointing vector for another body (such as the moon), replace the spacecraft coordinates with the coordinates of the other body.

The vector is calculated:

$$\hat{v}_x = -sc_{xyz}$$

$$\hat{v}_y = sun_{xyz} \times \hat{v}_x$$

$$\hat{v}_z = \hat{v}_x \times \hat{v}_y$$

Earth pointing angle is then derived:

$$A_{GCI} = A_q v$$

Pitch (θ) and yaw (ψ) for a 321 transformation are then:

$$\theta = \sin^{-1} -A_{13}$$

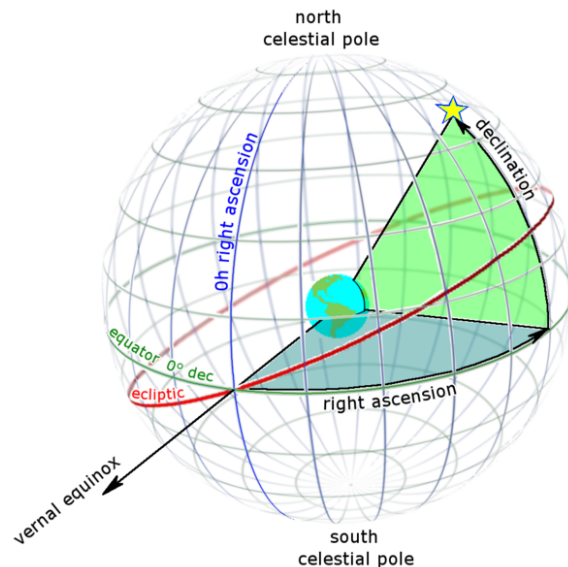
$$\psi = \tan^{-1} \frac{A_{23}}{A_{33}}$$

EPIC's field of view is approximately .5 degrees. However, these calculations are only for the center of an object; determining if an object is fully or partially outside the field of view requires knowing its angular size.

3.3 ASTRONOMICAL MODEL

The astronomical model describes the orientation of EPIC in regard to the Earth. This information is used to generate the 3D model, which is then in turn used to determine the per-pixel geolocation information.

Figure 4 - Depiction of right ascension and declination to a celestial object (depicted as a star) . Image from https://commons.wikimedia.org/wiki/File:%3ARa_and_dec_on_celestial_sphere.png



To determine the scene as seen by EPIC, it is necessary to perform astronomical calculations to determine Earth's celestial orientation during the time the image was taken. Initial right ascension (RA) and declination (DEC) values are calculated from a single point at the center of the Earth to the spacecraft and sun. These calculations are then adjusted for the Earth's orientation at the time of year and propagated across the surface, providing location-adjusted RA and DEC values. These values are then converted to azimuth and elevation values.

The math is the same for both the spacecraft and the sun, the only variance is the initial ephemeris coordinates used.

3.3.1 Right Ascension and Declination

The first step is to calculate the RA and DEC between the spacecraft the Earth's center.

Where x, y, z are the object coordinates in J2000 ephemeris reference frame:

$$\mathbf{hypot}_{xy} = \sqrt{x^2 + y^2}$$

$$\alpha = \tan^{-1} \frac{y}{x}$$

$$\delta = \tan^{-1} \frac{z}{\mathbf{hypot}_{xy}}$$

Where α is the right ascension and δ is declination. To convert right ascension from degrees to hour, divide it by 15.

3.3.2 Mean Sidereal Time

After this, it is necessary to calculate the apparent sidereal time, which is time as defined by the motion of the vernal equinox. The first step is to calculate the mean sidereal time, which is the sidereal without regards to Earth's nutation.

First, convert time to Julian days. The input is year, month, and decimal days. The output is "jd", julian days.

$$t = \text{year} + \frac{\text{month}}{100} + \frac{\text{day}}{10000}$$

if month ≤ 2 , then:

$$\text{year} = \text{year} - 1; \text{month} = \text{month} + 12$$

then continues:

$$\text{jd} = [365.25 * \text{year}] + [30.6001 * (\text{month} + 1)] + \text{day} 1720994.5$$

if $t \geq 1582.1015$, then:

$$i = \left\lfloor \frac{\text{year}}{100} \right\rfloor$$



$$i = 2 - i + \left\lfloor \frac{i}{4} \right\rfloor$$

$$jd = jd + i$$

The mean sidereal time (msrt) is then calculated:

$$t = \frac{(jd - 2451545.0)}{36525}$$

$$msrt = 280.46061837 + 360.98564736629 (jd - 2451545) + .000387933t^2 - \frac{t^3}{38710000}$$

and converted from degrees to hours.

3.3.3 Julian Dynamical Time

Julian Dynamical Time, also known as Julian ephemeris day (JDE), is the calculation of time without the fluctuations caused by Earth's rotation. It is needed for calculation nutation and precession. If JDE is not explicitly specified, use t as derived from Julian Day.

$$t = year - 2000$$

If year is 1986 or greater, and less than 2005:

$$\Delta T = 62.86 + 0.3345t - 0.060374t^2 + 0.0017275t^3 + 0.000651814t^4 + 0.00002373599t^5$$

If year is 2005 or greater, and less than 2050:

$$\Delta T = 62.92 + 0.33217t + 0.005589t^2$$

Then use the value of the Julian Day (jd), as calculated in 3.3.2 to calculate the Julian Ephemeris Day (jde):

$$jde = jd + \frac{\Delta T}{3600}$$

3.3.4 Nutation

It is then necessary to correct for nutation, the oscillation of Earth's rotational axis.



To calculate nutation, derive:

Calculate t with the Julian Ephemeris Day:

$$t = (jde - 2451545.0)/36525$$

The mean elongation of the Moon from the Sun:

$$D = 297.85036 + 445267.111480t - .0019142t^2 + \frac{t^3}{189474}$$

The mean anomaly of the Sun to Earth:

$$M = 357.52772 + 35999.050340t - .0001603t^2 + \frac{t^3}{300000}$$

The mean anomaly of the Moon:

$$MP = 134.96298 + 477198.867398t + .0086972t^2 + \frac{t^3}{56250}$$

The Moon's argument of latitude:

$$F = 93.27191 + 483202.017538 * t - .0036825 * t^2 + \frac{t^3}{327270}$$

The longitude of ascending node of the Moon's mean orbit on the ecliptic:

$$\omega = 125.04452 - 1934.136261t + .0020708t^2 + \frac{t^3}{450000}$$

Using the periodic terms defined in Appendix 6.1, calculate nutation in longitude ($\Delta\psi$) and the nutation in obliquity ($\Delta\epsilon$):

$$all_{arg} = D * d_{arg} + M * M_{arg} + MP * MP_{arg} + F * f_{arg} + \omega * \omega_{arg}$$

$$\Delta\psi = 0.0001 * \sum (sdelt_{arg} * t + \sin_{arg}) * \sin(all_{arg})$$

$$\Delta\epsilon = .0001 * \sum (cdelt_{arg} * t + \cos_{arg}) * \cos(all_{arg})$$

3.3.5 True Obliquity

Which is followed by a correction for the solar obliquity of the ecliptic, which is the angle between the ecliptic and the celestial equator.

Calculation of true obliquity:

$$\epsilon = 23^h26^m21.448_s - 21.448_s t - .00059_s t^2 + .001813_s t^3 + \Delta\epsilon$$



3.3.6 Apparent Sidereal time

The above calculations are put together then to derive the apparent sidereal time.

The correction to mean sidereal time is calculated:

$$\text{correction} = \frac{\Delta\psi}{15} + \cos \varepsilon$$

Which then yields the apparent sidereal time:

$$\text{asrt} = \text{msrt} + \frac{\text{correction}}{60}$$

3.3.7 Precession

Precession is an additional offset due to Earth's rotational reference frame being off axis. It has a period of ~26,000 years, but still has a significant enough effect to need to be calculated for this application.

Set jde equal to the Julian Ephemeris Day (3.3.3). Set jd0 equal to the J2000 epoch, the julian day on date 2000-01-01.5.

Then calculate:

$$T = (\text{jd0} - 2451545.0)/36525$$

$$t = (\text{jde} - \text{jd0})/36525$$

Then calculate:

$$\zeta = ((2306.2181 + 1.39656T - 0.000139T^2)t + (0.30188 - 0.000344T)t^2 + 0.018203t^3)/3600$$

$$z = ((2306.2181 + 1.39656T - 0.000139T^2)t + (1.09468 + 0.000066T)t^2 + 0.017988t^3)/3600$$

$$\theta = ((2004.3109 - 0.85330T - 0.000217T^2)t - (0.42665 + 0.000217T)t^2 - 0.041833t^3)/3600$$

The division by 3600 puts these values into units of degrees.

Then calculate, using the derived right ascension and declination (3.3.1):

$$A = \cos(\delta) \sin(\alpha + \zeta)$$

$$B = \cos(\theta) \cos(\delta) \cos(\alpha + \zeta) - \sin(\theta) \sin(\delta)$$

$$C = \sin(\theta) \cos(\delta) \cos(\alpha + \zeta) + \cos(\theta) \sin(\delta)$$

Then calculated the precession corrected right ascension and declination:



$$\alpha_p = \tan^{-1} \frac{A}{B} + z$$

$$\delta_p = \sin^{-1}(C)$$

3.3.8 Apparent Right Ascension and Declination

The apparent right ascension and declination are the right ascension and declination values corrected for the motion of the Earth's pole and equator. They are defined as:

$$\alpha_c = \alpha_p + \Delta\psi$$

$$\delta_c = \delta_p + \Delta\epsilon$$

This provides the angles between an object, such as the spacecraft, and the center of the Earth.

3.3.9 Parallax

If calculating for angles on the surface of the Earth, it is necessary to correct for parallax, the difference in apparent placement of an object due two different angles. This correction takes the apparent right ascension and declination values and converts them from Earth-centered angles to a series of angles specific to locations on the Earth's surface. The results are the topocentric right ascension and declination values.

The first step is to calculate the equivalent geocentric latitude coordinates for each geodetic latitude value (ϕ). These are defined as follows:

$$u = \tan^{-1} \left(\frac{B}{A} \tan \phi \right)$$

$$\rho \sin \phi' = \frac{B}{A} \sin u + \frac{H}{3678140} \sin \phi$$

$$\rho \cos \phi' = \cos u + \frac{H}{3678140} \cos \phi$$

Where A and B are the Earth's semi-major and semi-minor axis; H is the height at sea level.

It is then necessary to calculate the equatorial horizontal parallax via the following, where d is the distance to Earth:

$$\pi_h = \sin^{-1} \frac{\sin 8''.794}{d}$$

The geocentric hour angle is computed, in hours:

$$H_a = asrt - \frac{\lambda - \alpha_c}{15}$$



Then the right ascension correction for parallax is:

$$\Delta\alpha = \tan^{-1} \frac{-\rho \cos \phi' \sin \pi_h \sin H_a}{\cos \delta_c - \rho \cos \phi' \sin \pi_r H_a}$$

$$a' = a_c + \Delta\alpha$$

The declination correction for parallax is then calculated:

$$\delta' = \tan^{-1} \frac{(\sin \delta_c - \rho \sin \phi' \sin \pi_h) \cos \Delta\alpha}{\cos \delta_c - \rho \cos \phi' \sin \pi_h \cos H_a}$$

3.3.10 Azimuth and Elevation

The topocentric right ascension and declination values are then converted to azimuth and elevation angles using the following formulae.

$$azimuth = \tan^{-1} \frac{\sin H_a}{\cos H_a \sin \phi - \tan \delta \cos \phi}$$

$$elevation = \sin^{-1}(\sin \phi \sin \delta + \cos \delta \cos H_a)$$

After the azimuth and elevation angles are calculated for the entire globe, it is necessary to determine the orientation of Earth to the spacecraft at the time it was imaged. To do this, the elevation values of the 3D model are searched, and the nadir point is found. The latitude and longitude of this point is then used as the center point for the 3D to 2D projection.

3.4 2D TRANSFORM

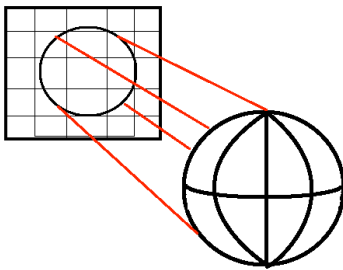


Figure 5 - Depiction of transforming the 3D model into the 2D plane

After the 3D model has been created, it is necessary to reproject the data into the 2D plane. The particular projection used is customized to the viewing geometry and sensor configuration of EPIC .

The transformation used is the EPIC Azimuthal Projection. It is not necessary to correct for the photographic nadir (tilted perspective), because EPIC's

narrow FOV requires a direct viewing angle, making this offset less than a pixel.

3.4.1 EPIC Azimuthal Projection

A previous version of geolocation (revision 04) used the perspective azimuthal projection. However, it was discovered that this projection does not appropriately handle



the distance distortion given the position of DSCOVER relative to Earth and EPIC's long focal length. A new projection was developed that dynamically calculates the correct pixel location and scale.

Assuming the WGS1984 geoid and the EGM2008 gravitational model, and that the spacecraft distance in meters (sd), latitude (ϕ), longitude (λ), and surface height (H) are known as:

Earth semi-major axis:

$$a = 6378137;$$

Earth semi-minor axis:

$$b = 6356752.314245;$$

Earth eccentricity:

$$e^2 = 6.69437999014e-3;$$

Earth sea-level elevation deviation:

H = EGM2008 gravitation model

The Earth's radius at latitude is defined as:

$$N = \frac{a}{\sqrt{1 - e^2 \sin^2 \phi}}$$

The body is then defined as:

$$\begin{aligned} Z &= (N + h) \cos \phi \cos \lambda \\ X &= (N + h) \cos \phi \sin \lambda \\ Y &= (N(1 - e^2) + h) \sin \phi \end{aligned}$$

The rotation angles are defined as:

$$\begin{aligned} r_x &= \delta_c \text{ (apparent declination 3.3.8)} \\ r_y &= \phi_{90} \text{ (latitude at view elevation angle } 90^\circ) \\ r_z &= \phi \text{ (spacecraft roll angle 3.2.3)} \end{aligned}$$

Rotation into true of day coordinates:

$$\begin{aligned} Z_y &= Z \cos(r_y) - X \sin(r_y) \\ X_y &= Z \sin(r_y) + X \cos(r_y) \\ Y_x &= Y \cos(r_x) - Z_y \sin(r_x) \end{aligned}$$



$$\begin{aligned}
Z_{tod} &= Y \sin \phi_0 + (Z \cos -\lambda_0 - X \sin -\lambda_0) \cos \phi_0 \\
X_{tod} &= (Z \sin -\lambda_0 + X \cos -\lambda_0) \cos \psi_0 - (Y \cos \phi_0 - Z \sin \phi_0) \sin \psi_0 \\
Y_{tod} &= (Z \sin -\lambda_0 + X \cos -\lambda_0) \sin \psi_0 + (Y \cos \phi_0 - Z \sin \phi_0) \sin \psi_0
\end{aligned}$$

Conversion into image coordinates, where f is the telescope focal length and x_offset and y_offset are defined as the center point offset of the Earth in the image:

$$\begin{aligned}
x &= \frac{f X_{tod}}{\left(\sqrt{(dist - Z_{tod})^2 + X_{tod}^2 + Y_{tod}^2} - f \right) ccd_size} + x_offset \\
y &= \frac{f Y_{tod}}{\left(\sqrt{(dist - Z_{tod})^2 + X_{tod}^2 + Y_{tod}^2} - f \right) ccd_size} + y_offset
\end{aligned}$$

The above coordinates contain values that are not viewable by EPIC, i.e., the opposite side of the Earth. To clip these values out of the model, calculate:

$$c = \tan^{-1} \frac{Z_{tod}}{\text{hypot}(X_{tod}, Y_{tod})}$$

$$x = x \cup (c > 0)$$

$$y = y \cup (c > 0)$$

3.4.2 Atmospheric Refraction

EPIC views a wide swath of the Earth, which makes the geolocation susceptible to atmospheric refraction. With atmospheric refraction, light bends as it enters and exits the atmosphere, acting as a lens and distorting the location of objects on Earth. Figure 6 shows an example.

It is necessary, particularly at large zenith angles to correct for this. As part of the geolocation, these angles are corrected and used for computing the actual latitude and longitudes observed. The angles are not added to the zenith angle in the product;

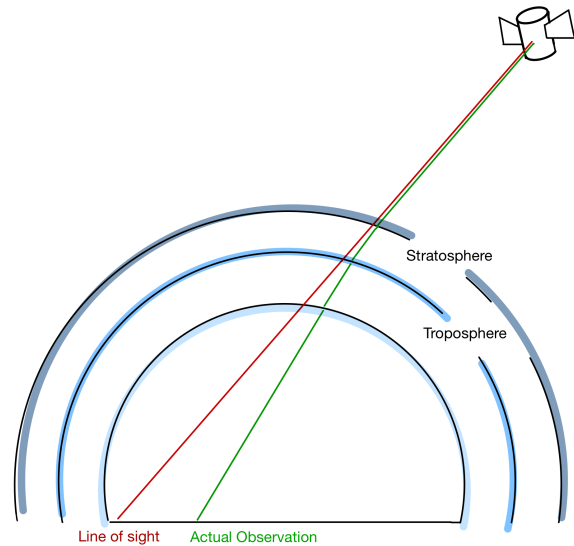


Figure 6 - Example of atmospheric refraction. The red line is the spacecraft's direct line of sight, the green line is what it actually observes



however, they are left as a separate product.

The algorithm to calculate the atmospheric refraction accurately across the disk is complicated, and it is not possible to accurately convey the math and reasoning without reproducing the paper in its entirety. The paper, including demonstration source code, can be found under Hohenkerk in References (8).

3.4.3 Area Mapping

In order to remap the coordinates above into the image, a remapping method used which is called “area mapping”. Doing a direct, non-linear transformation, with a straight pixel-to-pixel mapping provides poor results – pixels are clustered, with multiple pixels colliding for the same remapped space, and conversely gaps where no pixels fill the solution. To avoid this problem, an area-mapping algorithm is used instead. In area mapping, each pixel is assumed to occupy a 2D space, as opposed to a single 1D point. In the mapping process, the 2D shape of the pixel is retained until the transform is completed, and then the data is regridded, with each portion of the original pixel reassigned proportionally to the pixels it matches.

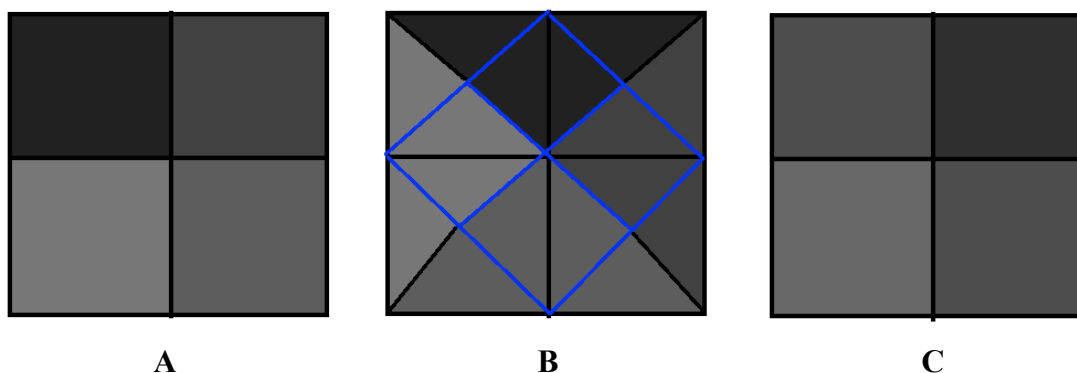


Figure 7 - Example of a coarse resolution area mapping. A) is the original pixel orientation; B) the original pixels (blue) shown in their new orientation after transformation; C) Remapped pixels

This pixel mixing does add a small amount of smoothness to the data, estimated to be at about 2%, but the correlation to the original data is consistent over the entire image. This is unlike the static pixel mapping, where clusters of pixels will have high correlation to the original data and other clusters, which require interpolation to fill missing areas, will have low correlation to the original data.

To make the algorithm computationally efficient, the data is broken into subpixels.

For an image i with coordinates x, y , that has been divided into N subpixels with coordinates x, y , the following remapping formula is used.



$$i_{xy} = \frac{1}{N^2} ((N-x)(N-y)i_{x,y} + x(N-y)i_{x,y+1} + y(N-x)i_{x+1,y} + xyi_{x+1,y+1})$$

A straightforward way to calculate this on a computer is to generate a mask of valid i values, known as m . Both i and m are resampled to scale N using nearest neighbor interpolation. The transformation is then applied to the rescaled image I , and mask m . The image and mask are then down sampled to the original resolution using bilinear interpolation. This results in the down sampled image containing the mean value of the subpixels, and the down sampled mask containing the weight of the number of valid subpixels. The down sampled image is then divided by the down sampled mask to produce the area mapped image.

3.4.4 Optical Correction

EPIC has a small barrel distortion and a tangential skew that requires correction. The terms of the distortion are described, in this version of the software, as follows.

Radial coefficients:

$$\begin{aligned} K_1 &= 0 \\ K_2 &= -8.84353741496599e^{-18} \\ K_3 &= 2.51700680272109e^{-24} \end{aligned}$$

Tangential coefficients:

$$\begin{aligned} P_1 &= 1.82585034013606e^{-7} \\ P_2 &= -1.94761904761905e^{-7} \\ P_3 &= 2.59911564625851e^{-7} \\ P_4 &= -4.94897959183673e^{-14} \end{aligned}$$

Linear offsets:

$$\begin{aligned} x_c &= -342.31156462585 \\ y_c &= -256.039455782313 \end{aligned}$$

The equation that describes the distortion is as follows. The pixel coordinates are defined as x , the pixel column, and y , the pixel row.

Calculate the delta between the physical CCD center and the optical center:

$$\begin{aligned} \Delta x &= x - x_c \\ \Delta y &= y - y_c \end{aligned}$$

Radial distance:

$$r = \sqrt{\Delta x^2 + \Delta y^2}$$

The pixel offset, according to the optical model, is then:

$$x' = \Delta x + (K_1 r^2 + K_2 r^4 + K_3 r^6) + P_1 (r^2 + 2\Delta x^2) + 2P_2 (\Delta x \Delta y) (1 + P_3 r^2 + P_4 r^4)$$



$$y' = \Delta y + (K_1 r^2 + K_2 r^4 + K_3 r^6) + 2P_1(\Delta x \Delta y) + P_2(r^2 + 2\Delta y^2)(1 + P_3 r^2 + P_4 r^4)$$

Using this formulation, it is possible to either add or remove the optical distortion. Optical distortion is added to the geolocation model in L1A, which permits the L1A images to be geolocated but unmodified. In the L1B, the optical distortion is removed from the images.

3.4.5 Subpixel Correction

To improve correlation of the data after the initial L1B images are generated, a subpixel correction is applied. A series of correlation tests are performed between an image and a reference image in which each test has a slight 2D transformation applied to it. The results of these tests are scored, and the one with the best correlation score against the reference image has that translation applied.

The reference image used is defined by rank; if the first choice is missing from a set, the next one in the set is selected. The rank is defined by which bands correlate best to the others. 443nm has the highest correlation; it's also the only band sampled at the full resolution.

The rank is as follows:

Table 1 - Ranking of suitability for bands to be used as reference band in subpixel correction

Rank	Band (nm)
1	443
2	551
3	680
4	688
5	764
6	780
7	388
8	340
9	325
10	317

To determine the level of correlation between the bands and the reference bands, the following calculation, which determines the Pearson correlation coefficient, is used.

Assuming A and B are images, the score, or correlation is calculated as:

$$a = A - \text{mean}(A)$$

$$b = B - \text{mean}(B)$$



$$r = \frac{\sum(a * b)}{\sqrt{\sum a^2 b^2}}$$

The above is applied using the multi-tiered search algorithm. In the search algorithm, the transformation is constrained by user inputted values consisting of an xy offset and a shifting range and shifting size. The image is translated for every set generated by the constraint, and the correlation score is calculated, identifying the best xy offset in this set. This is done for at coarse, medium, and fine resolutions – the returned xy offset is fed into the following finer grain analysis. This multi-tiered approach permits calculations to be done at the subpixel level while minimizing the computational intensity.

3.5 CORRECTION FOR ATTITUDE ERROR

The star tracker on DSCOVR has a roll accuracy less than .5 degrees. EPIC images require .05 degrees to achieve half pixel accuracy. The correction for this requires an iterative process that uses the above astronomical and instrument calculations to draw MODIS data into simulated EPIC images. These images are then compared for the correction.

The steps for this process are as follows:

- 1) Using the initial Earth centering, astronomical, and attitude values calculated in sections 3.1, 3.2, and 3.3 and the 2D transformation algorithm described in 3.4, MODIS data is redrawn into a simulated EPIC image in the same pose as the EPIC image being geolocated.
- 2) Additional images are generated using a coarse spread of values that represent the known range of attitude error.
- 3) The simulated images are evaluated against the original EPIC image using the Pearson Correlation Coefficient (described in 3.4.5). This produces a “score” that informs the program how well the simulated image correlates against the original.
- 4) The image with the best score is selected, and the inputs are used to generate another simulated image. The process repeats, using a finer resolution spread on the inputs. It will continue until the results converge. This corrected attitude is then used to generate the final geolocation solution.

This process produces results that brings the geolocation solution within requirements. The use of the entire image, instead of focusing on coastal edges as other algorithms do, permits decent solutions for images where there is little land mass, such as in the Pacific.

3.6 LEVEL 1A ALGORITHM

The Level 1A algorithm produces geolocated images and maintains the original calibrated EPIC image. This means that the image is left unmodified, and the latitude, longitude, and associated angles are instead transformed into the frame of the image.



The mathematical formulas and algorithms in the above section are combined as follows to produce the L1A.

- 1) Attitude Determination – Determines object pointing at and rotational correction
- 2) Image Registration – the XY Earth centering coordinates are calculated
- 3) Astronomical Model – 3D model is generated with viewing/sun geometry for whole Earth
- 4) 2D Transformation (Model) – Calculates the corresponding XY image coordinates to the model in the image's original view frame. Applies centroid and rotational offsets. Data is remapped using direct transformation (XYZ->XY).
- 5) Optical Model – Optical offsets are applied to location and view angle datasets
- 6) Correction for Attitude Error – Calculates correction for star tracker error.
- 7) Generate archive – Metadata is collected, and data is stored to HDF

3.7 LEVEL 1B ALGORITHM

In the level 1B algorithm, all image bands in a set are transformed into the same reference frame. This involves rotating the images so that north is up, as well as correcting the 3D geometry for Earth's rotation over the time of the viewing period. The mathematical formulas in the previous sections are combined as follows to produce the L1B. Note that this is largely similar to the L1A, the primary difference is the use of the reference geometry in the calculations instead of the image's native geometry and that the L1B image has been transformed into the reference geometry.

- 1) Reference Geometry Selection – The reference image is selected, based on the image taken in the middle of the sequence
- 2) 3D Model Import – Pulls in the relevant data from the L1A file
- 3) Astronomical Model – Calculates viewing geometry for reference frame, but at the unique time for each image
- 4) 2D Transformation (Image) – Calculates the corresponding XY image coordinates to the model in the reference view frame. This results in applying the 3D rotational correction, optical correction, and XY transform in one step. Image is remapped using the area mapping algorithm.
- 5) 2D Transformation (Model) – Calculate the corresponding XY image coordinates to the model in the reference view frame. Applies centroid and rotational offsets. Data is remapped using direct transformation (XYZ->XY).
- 6) Generate archive – Metadata is collected, and data is stored to HDF

3.7.1 Multi-day alignment

The L1B algorithm, in addition to providing geographic correction for an EPIC 10-band set, can also be used to geographically align images taken on different days. The same algorithm as the L1B is used, with a fixed reference geometry used for all the images across multiple days. This is somewhat of an extreme example of how the L1B algorithm functions, as in its typical utilization corrections are usually under 10 pixels.



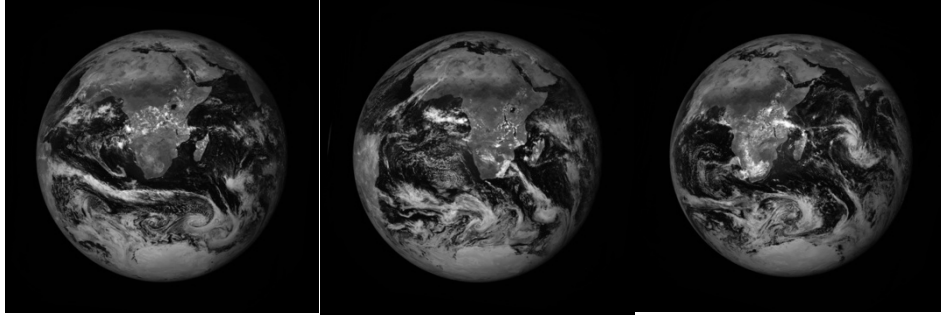


Figure 8 - Original images, native geometry



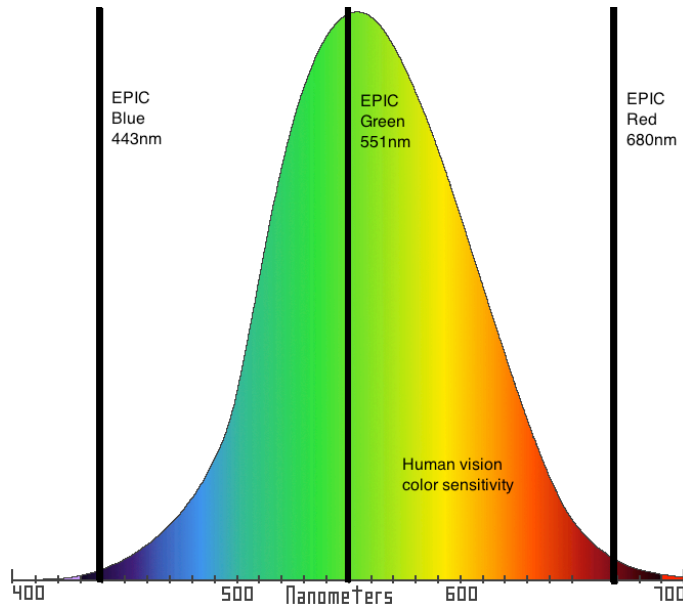
Figure 9 Above images reprojected to same geometry



4 COLOR IMAGERY

In addition to geolocation, the level 1 processing produces a color image. The processing used is a derivative of the International Commission on Illumination (CIE) process for estimating tristimulus values from calibrated instruments.

The spectral range for EPIC's 10 bands run from 317nm-780nm. Human vision ranges from 400-700nm. Although there is considerable overlap between the two, EPIC and humans view the spectrum very differently. EPIC samples the spectrum in 10 narrow bands at effectively equal brightness per band. The human eye samples the spectrum in 3 wide ranges, overlapping bands with varying sensitivity at different parts of the spectrum.



To reconcile these two requires a transformation from EPIC's view to human viewable "natural color image". There are three steps required to do this. The first is to convert the level 1b from values of counts per second into reflectance using the calibration factors provided by the EPIC science team. Secondly, it is necessary to provide a small correction for brightness related to Rayleigh scattering, as the blue and red band are out the outer skirts of the human vision and this upsets the color balance due to the difference in scattering between what EPIC sees and a person would see. The thirdly, it is necessary to rebalance the bands such that they match how the human eye perceives the spectrum. Fortunately for the third step, there is an established methodology used in industry, for taking the precise, abstract, data from calibrated instruments and converting them into the red, green, and blue values that compromised human vision. Using this it is possible to take EPIC's multi-spectral imagery and produce natural color images.



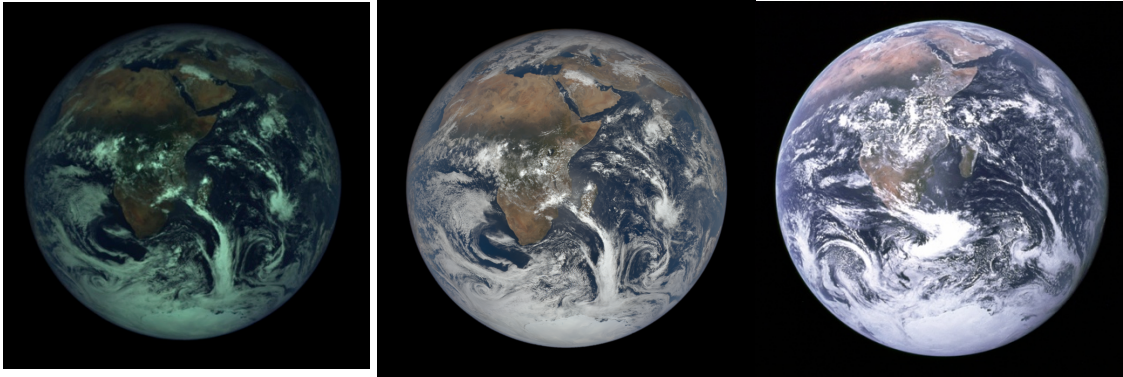


Figure 10 – 3 Earths: Uncorrected EPIC; color corrected EPIC; Apollo 17 blue marble

4.1 RAYLEIGH SCATTERING

Rayleigh scattering is a wavelength dependent illumination effect that is stronger in the blue/UV part of the spectrum than it is in other visible channels. Light striking the atmosphere scatters, causing the blue color of the sky, but its effect is seen at all wavelengths. It is strongest at large viewing angles, causing the white, washed-out affect near the edges of the Earth in EPIC imagery.

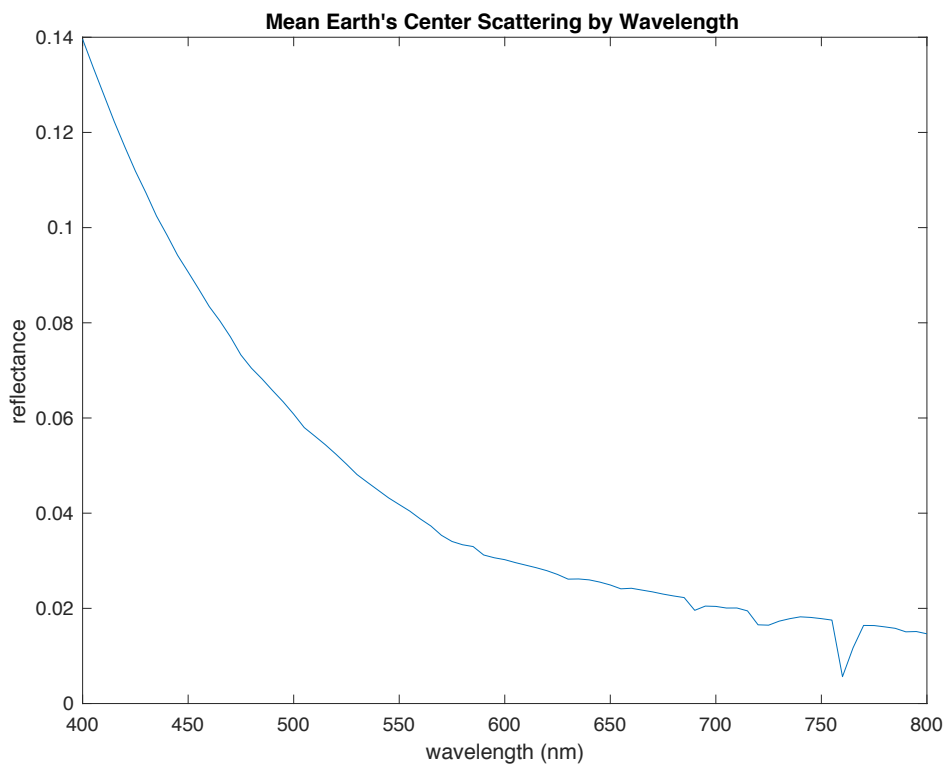


Figure 11 - Amount of scattering in center of Earth from EPIC's field of view, by wavelength



This effects the generation of the color images, as EPIC samples blue at 443nm, which is actually in the violet range of color perception. The human range of blue is within 450-485nm. When accounting for blue sensitivity and the amount of scattering in 443nm, there is about 15% difference in brightness between what is measured and what a human would perceive, if this was an actual blue channel. This results in a loss of contrast, as well as an increased blueness in the EPIC images.

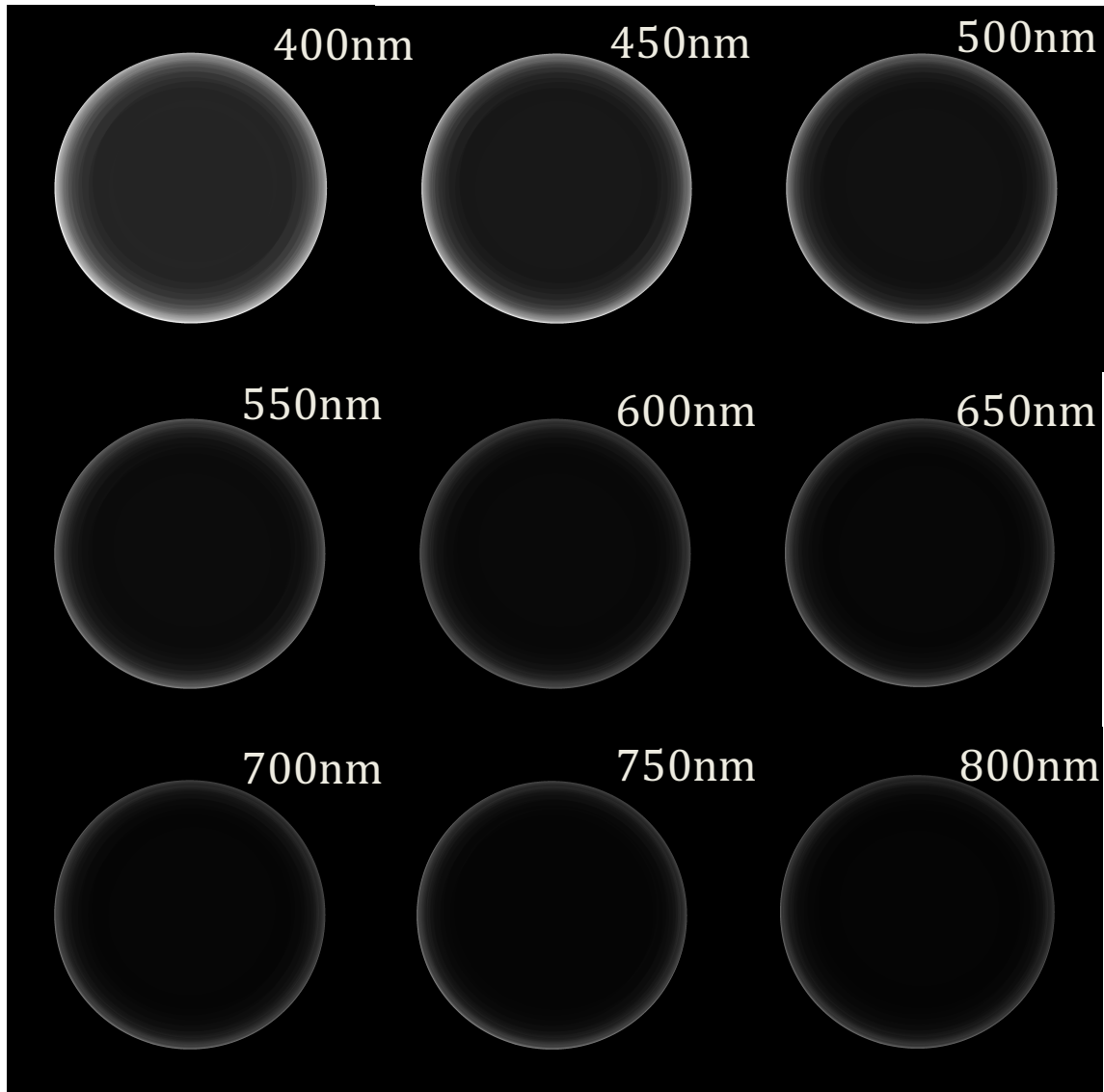


Figure 12 - Rayleigh scattering calculated at different wavelength across the surface of the Earth in EPIC images.

Previous versions of the color algorithm used a heuristic to compensate for this. This version introduces a correction for the bias created by Rayleigh scattering across all bands. The result is an image with more accurate contrast and a reduction of blue in the image. In the new image, the difference is very small, as the original algorithm's heuristic



reasonable compensated for this issue. The intention of this change is to provide an algorithm that is more mathematically complete and accurate.

4.2 CIE COLOR SYSTEM

Different types of color system are used for different mediums. Computers monitors use a ratio of Red/Green/Blue (RGB); printers use Cyan/Magenta/Yellow/Key (CYMK). CIE uses an XYZ coordinate system than encompasses a broader range of colors than the former two.

Calculating the CIE XYZ coordinates requires knowing 3 values. At a particular wavelength, what is the measured intensity of the object, the spectral intensity of the light source, and the human visual sensitivity at this spectrum. It is mathematically defined as:

$$X = k \sum_{\lambda=360}^{\lambda=830} E(\lambda) \bar{x}(\lambda) P(\lambda)$$

$$Y = k \sum_{\lambda=360}^{\lambda=830} E(\lambda) \bar{y}(\lambda) P(\lambda)$$

$$Z = k \sum_{\lambda=360}^{\lambda=830} E(\lambda) \bar{z}(\lambda) P(\lambda)$$

Where λ , is the spectral wavelength, k is a normalization factor, $E()$ is the illuminant, $P()$ is the reflectance of the object, and XYZ is the CIE human vision color matching coordinates.

The above effectively integrates the instrument measurement, lighting conditions (illuminant), and human sensitivity over the range of human vision, providing a coordinate that identifies the color measured.

The CIE provides illuminant and color-matching functions in tables of 1 or 5nm resolution.

In order to compensate for the differences in Rayleigh scattering across the wavelengths, an additional correction must be appended. This is delta R, which is the difference in Rayleigh scattering in the center of Earth between the band used as reference and the wavelength being integrated on. The values of R can be found in section 6.2.

The XYZ values as calculated for EPIC are:

$$X = k \sum_{\lambda=360}^{\lambda=830} E(\lambda) \bar{x}(\lambda) P(\lambda) \Delta R(\lambda)$$

$$Y = k \sum_{\lambda=360}^{\lambda=830} E(\lambda) \bar{y}(\lambda) P(\lambda) \Delta R(\lambda)$$



$$Z = k \sum_{\lambda=360}^{\lambda=830} E(\lambda) \bar{z}(\lambda) P(\lambda) \Delta R(\lambda)$$

Where λ , is the spectral wavelength, k is a normalization factor, $E()$ is the illuminant, $P()$ is the reflectance of the object, $\Delta R(\lambda)$ is the difference in Rayleigh scattering from the reference band, and XYZ is the CIE human vision color matching coordinates.

For the DSCOVER imaging, the D65 illuminant is used. This is the illuminant that resembles “mid-day light” on Earth. Of course, DSCOVER is not on Earth, which modifies the nature of the illuminant, as the light is not filtered through the atmosphere. However, the human eye has very weak spectral response to frequencies that are filtered by the atmosphere; when considering the response-weighted impact of D65 versus unfiltered sunlight, plus the truncation to 24-bit RGB color space, the difference is minimal. There are 2 possible choices for color matching tables – CIE 1931 and 1964. CIE1964 is used here, as it is recommended for objects that encompass a larger field of view.

In order to implement the above algorithm, there are two additional steps that are necessary. The first is the need to normalize the bands according to the width of their spectral sensitivity. This is implemented by the Stearns-and-Stearns correction, which is applied to each sampled band as:

$$P_i = .083P'_{i-1} + (1 + .166)P'_i - .083P'_{i+1}$$

With the exception of the first and the last band where it is:

$$P_i = (1 + .083)P'_i - .083P'_{i+1}$$

After this normalization is done, it is necessary to fill in the missing parts of the spectrum. This is done via linear interpolation. The bands 340nm, 388nm, 443nm, 551nm, 680nm, 764nm, and 780nm are used. 688nm, although within the visual range is left out. As an absorptive band, the images are very dark and low detail.

After the tristimulus values are calculated for each pixel, it is necessary to convert them to RGB for display. The conversion from XYZ to sRGB is defined as:

$$\begin{bmatrix} R \\ G \\ B \end{bmatrix} = \begin{bmatrix} 3.2406 & -1.5372 & -.4986 \\ -.9689 & 1.8758 & .0415 \\ .0557 & -.2040 & 1.0570 \end{bmatrix} \begin{bmatrix} X \\ Y \\ Z \end{bmatrix}$$

The final correction is for brightness. There are two parts, gamma correction and exposure. Gamma correction is the conversion from linear brightness space to human brightness sensitivity, which follows a power-law function. sRGB gamma correction scheme follows a .45 curve. Previous to this version, a gamma correction of .7 was used, which helped offset the loss of contrast due to Rayleigh scattering in 443nm.



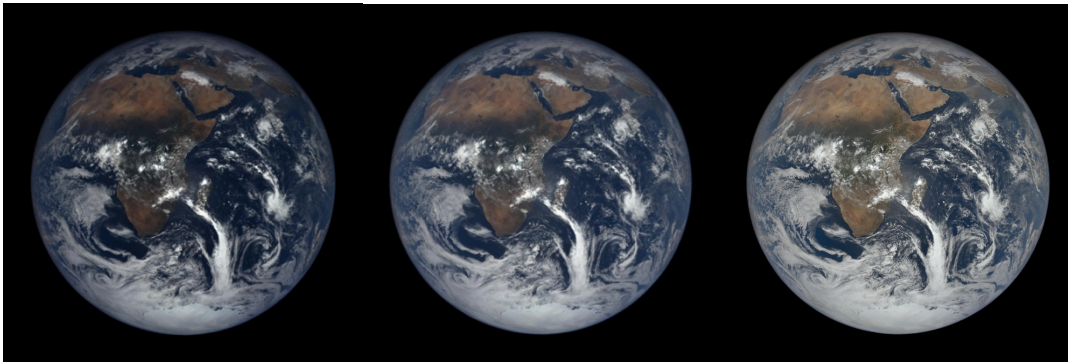


Figure 13 - No gamma correction; Gamma correction from previous version; sRGB gamma with Rayleigh correction

Exposure correction is the only element that does not have an easy mathematical correlation to human vision. This is because the human eye constantly, dynamically changes its exposure through pupil dilation as it views a scene. Photographs, on the other hand, have a single, fixed exposure. Many conventional space photographs, including the famous Apollo 17 blue marble, choose to expose for land, resulting in saturated, featureless clouds. However, the clouds are far brighter in the original EPIC data. Even in the red band, which features land the best, the clouds are about 4.25x brighter than the land or $\sim 2.7x$ on the power law scale.

It is very clear between this and from reading the Apollo transcripts that the land-enhanced view does not represent a natural view of space, as in the transcripts the quality and nature of clouds are described in high detail.

To this end, an exposure enhancement is applied which results in the top 15% brightest pixels are saturated. This number was derived empirically based on the brightest the image could be without saturating the eye of a hurricane.

The resulting images were found to be comparable to space shuttle and space station digital photography. Some caution needs to be applied making comparisons to film photography, particularly during the Apollo era. Although the cameras utilized ultraviolet filters, the film used, Kodak Ektachrome SO-168, was still overly sensitive in the blue range. Although there were attempts made in correcting for this in post processing, such as for the Apollo 17 blue marble, many of the online galleries features digital scans of the negatives without correction.



5 ALGORITHM OUTPUT

The L1A and L1B geolocation results are stored in Hierarchical Data Format 5 files. For information specific to the format of the files, please refer to the “EPIC Data Format Control Book”.

The data is grouped into “viewing periods”. A “viewing period” consists of a time period less than 15 minutes in which a set of different bands has been taken. In nominal operations, a viewing period is within 8 minutes and consists of 10 bands, or one image per filter.

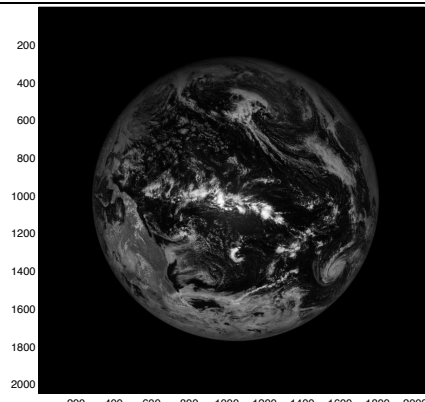
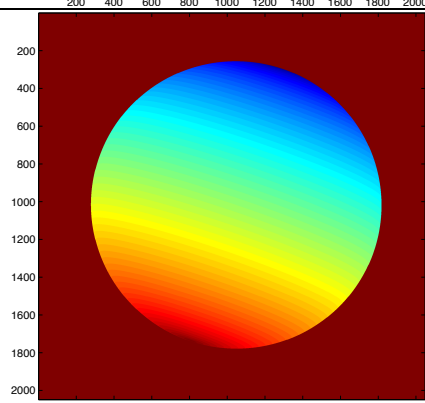
L1A and L1B files have largely the same structure, but the contents are different. At the root is a list of all bands. Each band is placed in its own group and has associated geolocation information with it. The contents are as follows.

5.1 LEVEL 1A

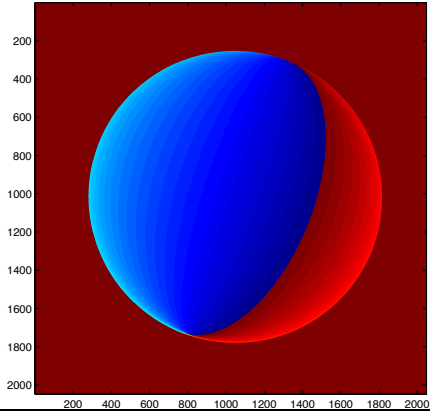
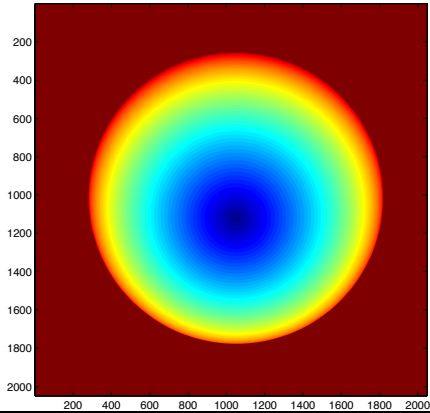
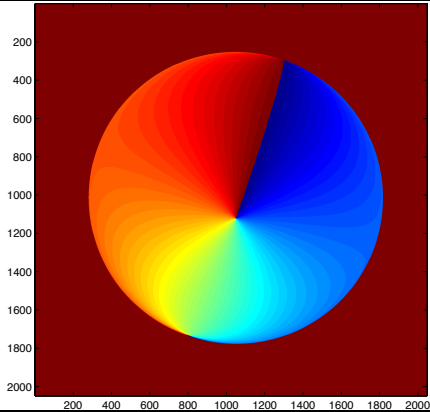
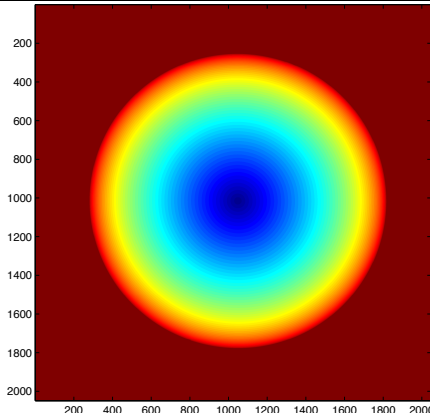
Level 1A product contains a calibrated image in its native orientation as it was taken on the spacecraft. Geolocation information is appended and aligned to be in the image’s native orientation. For more information on the L1A calibration, refer to the “L1A Calibration Definition”.

5.1.1 Band Group

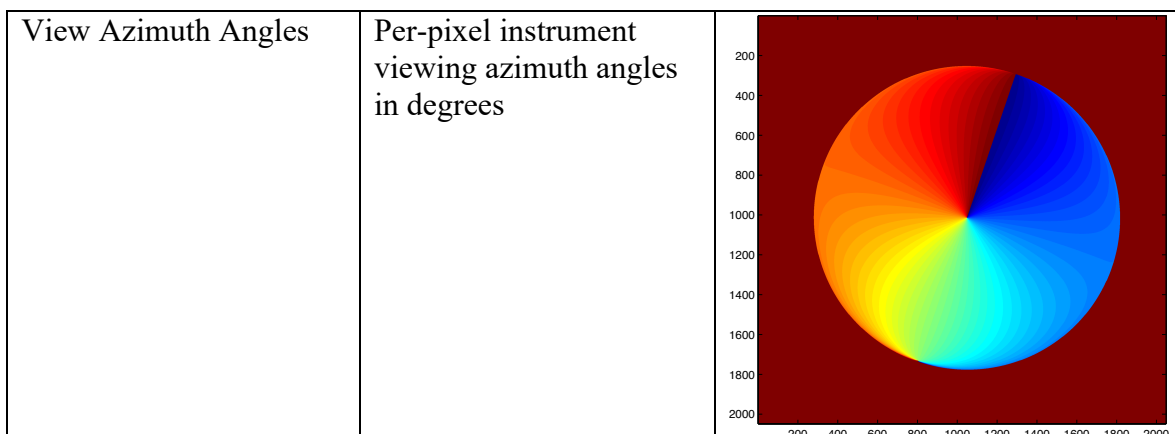
Each band group consists of the following.

Image	Calibrated level 1A image in native orientation	
Latitude	Per-pixel latitude values in degrees	

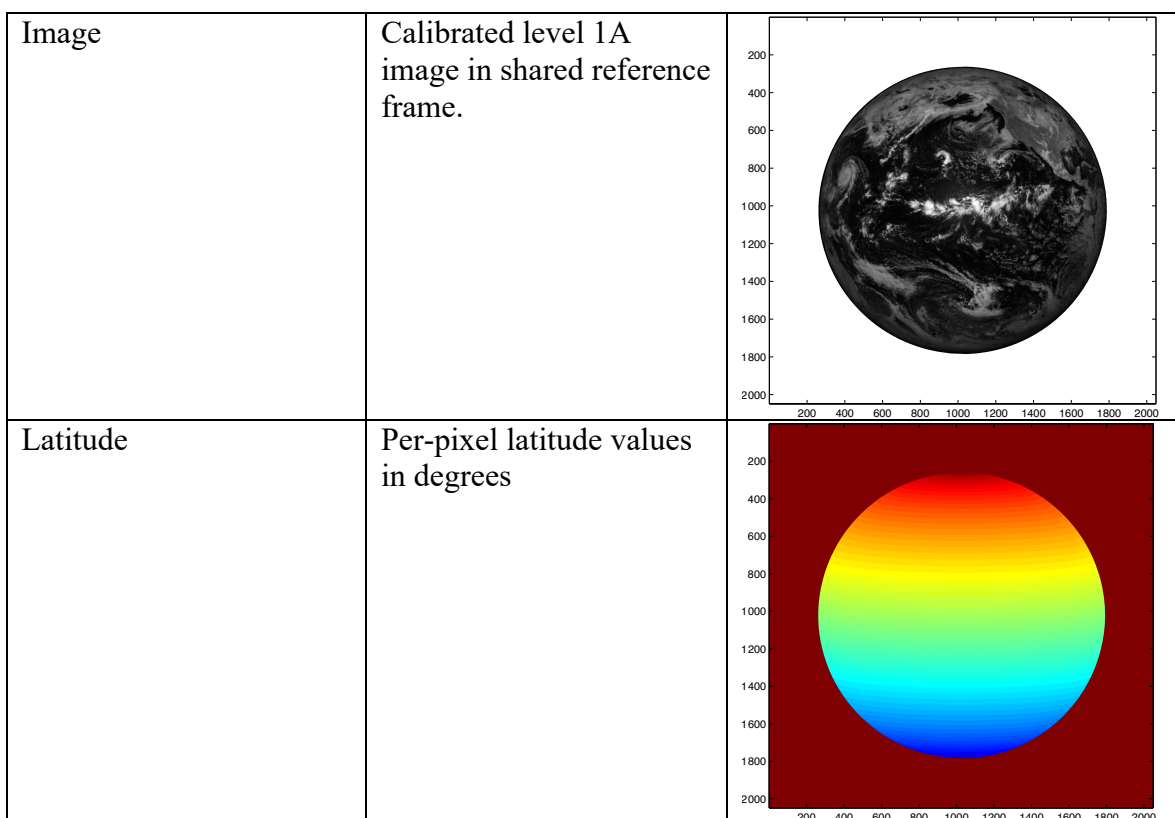


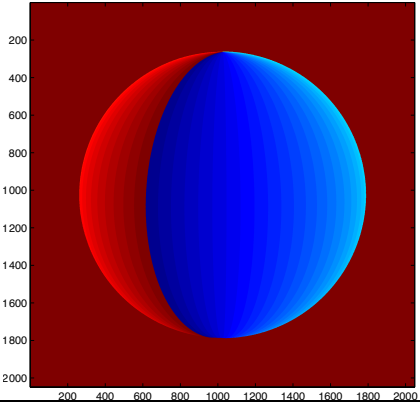
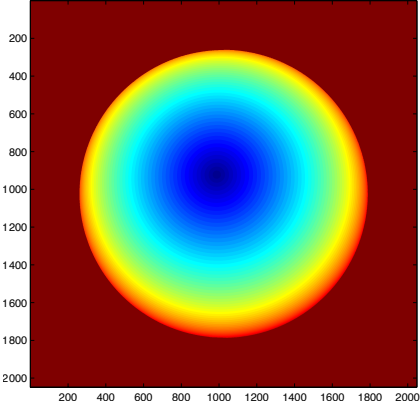
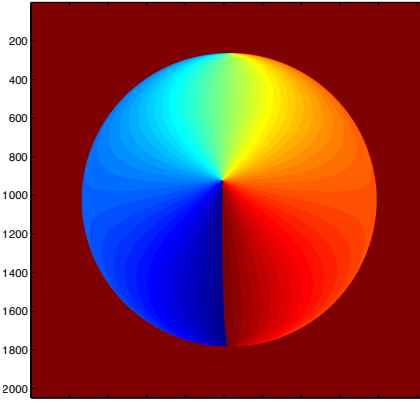
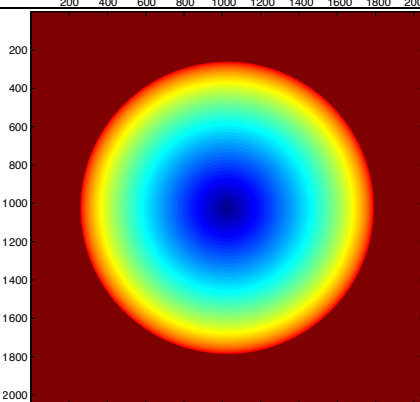
Longitude	Per-pixel longitude values in degrees	
Sun Zenith Angle	Per-pixel sun zenith angles in degrees	
Sun Azimuth Angle	Per-pixel sun azimuth angles in degrees	
View Zenith Angles	Per-pixel instrument viewing zenith angles in degrees	



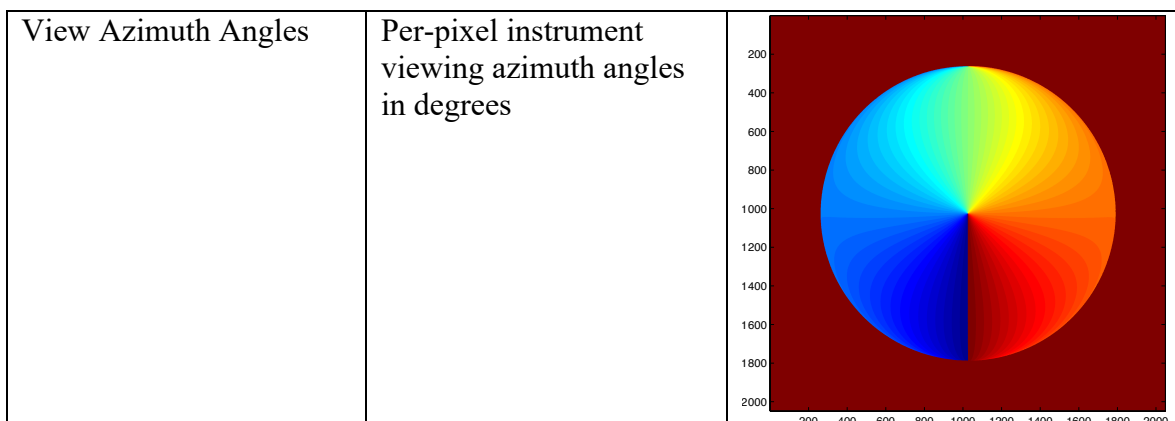


5.2 LEVEL 1B



Longitude	Per-pixel longitude values in degrees	
Sun Zenith Angle	Per-pixel sun zenith angles in degrees	
Sun Azimuth Angle	Per-pixel sun azimuth angles in degrees	
View Zenith Angles	Per-pixel instrument viewing zenith angles in degrees	





The level 1B contains the same types of datasets as the level 1A, however these have been corrected so that all images and ancillary data share the same reference geometry. This includes correcting for X/Y translation offsets due to spacecraft jitter, rotation for North to be “up” in the image, and correction for Earth’s rotation over the viewing period.

5.3 GEOLOCATION METADATA

The same geolocation metadata is available for both the L1A and L1B data. The table below contains information regarding the contents of the metadata and appropriate references.

<i>apparent_sidereal_time</i>	Apparent sidereal time for the hour angle of the vernal equinox. As calculated in section 3.3.6
<i>attitude_quaternion_0</i> , <i>attitude_quaternion_1</i> , <i>attitude_quaternion_2</i> , <i>attitude_quaternion_3</i>	Interpolated attitude quaternions as obtained from star tracker. These are not corrected for off pointing/roll. As calculated in section 3.2.2
<i>bottom_latitude</i> , <i>bottom_longitude</i> , <i>left_latitude</i> , <i>left_longitude</i> , <i>right_latitude</i> , <i>right_longitude</i> , <i>up_latitude</i> , <i>up_longitude</i>	Latitude/Longitude coordinates closest to various image sides
<i>centroid_center_latitude</i> , <i>centroid_center_longitude</i>	Latitude and longitude reflecting center of projection; approximately 0 degree viewing zenith angle
<i>centroid_polar_pixel_size</i>	Size of Earth from North to South pole in pixels. As calculated in section Error! Reference source not found.
<i>centroid_x_pixel_offset</i> , <i>centroid_y_pixel_offset</i>	X/Y offset required to translate Earth to the center of the image. As calculated in section 3.1.3
<i>dscovr_declination</i> , <i>dscovr_right_ascension</i>	DSCOVr declination and right ascension angles in respect to Earth. As calculated in section 3.3.1
<i>dscovr_ephemeris_x_position</i> , <i>dscovr_ephemeris_y_position</i> , <i>dscovr_ephemeris_z_position</i> , <i>dscovr_ephemeris_x_velocity</i> , <i>dscovr_ephemeris_y_velocity</i> , <i>dscovr_ephemeris_z_velocity</i>	The interpolated J2000 ephemeris coordinates for DSCOVr at imaging time
<i>earth_north_direction</i>	Rotational angle required to rotate Earth so



	North is up. As calculated in section 3.2.3
<i>lunar_ephemeris_x_position,</i> <i>lunar_ephemeris_y_position,</i> <i>lunar_ephemeris_z_position,</i> <i>lunar_ephemeris_x_velocity,</i> <i>lunar_ephemeris_y_velocity,</i> <i>lunar_ephemeris_z_velocity</i>	The interpolated J2000 ephemeris coordinates for the Moon at imaging time
<i>north_latitude,</i> <i>east_longitude,</i> <i>south_latitude,</i> <i>west_longitude</i>	Coordinate boundaries of Earth in image
<i>solar_declination,</i> <i>solar_right_ascension</i>	Sun declination and right ascension angles in respect to Earth. As calculate in section 3.3.1
<i>solar_ephemeris_x_position,</i> <i>solar_ephemeris_y_position,</i> <i>solar_ephemeris_z_position,</i> <i>solar_ephemeris_x_velocity,</i> <i>solar_ephemeris_y_velocity,</i> <i>solar_ephemeris_z_velocity</i>	The interpolated J2000 coordinates for the Sun at imaging time





6.1 PERIODIC TERMS FOR CALCULATION OF NUTATION

6.2 RAYLEIGH CORRECTION FACTOR

<https://www.mdpi.com/2072-4292/10/4/560>

The calculated values of R are a simplified version of what was provided in the paper – these are Rayleigh correction factors for the center field of view of EPIC images.

Wavelength	Rayleigh (R)
400	0.1396
405	0.1337
410	0.128
415	0.1223
420	0.117
425	0.1119
430	0.1073
435	0.1024
440	0.0984
445	0.0942
450	0.0907
455	0.0871
460	0.0834
465	0.0804
470	0.0771
475	0.0732
480	0.0705
485	0.0682
490	0.0658
495	0.0634
500	0.0608
505	0.058
510	0.0562
515	0.0544
520	0.0524
525	0.0503
530	0.0481
535	0.0465
540	0.0448
545	0.0432
550	0.0418
555	0.0404
560	0.0388
565	0.0373
570	0.0354
575	0.0341
580	0.0334



585	0.033
590	0.0312
595	0.0306
600	0.0302
605	0.0296
610	0.0291
615	0.0285
620	0.0279
625	0.0271
630	0.0261
635	0.0262
640	0.026
645	0.0255
650	0.0249
655	0.0241
660	0.0242
665	0.0238
670	0.0235
675	0.023
680	0.0226
685	0.0223
690	0.0196
695	0.0205
700	0.0204
705	0.0201
710	0.0201
715	0.0195
720	0.0165
725	0.0165
730	0.0173
735	0.0178
740	0.0182
745	0.0181
750	0.0178
755	0.0175
760	0.0056
765	0.0117
770	0.0164
775	0.0164
780	0.0161



785	0.0158
790	0.0151
795	0.0151
800	0.0147

7 REVISION UPDATES

7.1 UPDATES FROM REVISION 4 TO 5

Improvements for this revision include:

- Improved focal length estimation.
- New 3D-2D projection algorithm
- Use of anti-aliasing to reduce data artifacts
- Improved geoid model

7.2 UPDATES FROM REVISION 5 TO 6

Improvement for this revision include:

- Correction for Star Tracker uncertainty
- Improved optical model, including new geometric correction
- Atmospheric refraction calculation

8 REFERENCES

Astrobaki, *Coordinates*. <https://casper.berkeley.edu/astrobaki/index.php/Coordinates>, May 4, 2016

Billmeyer, Fred. *Principles of Color Technology*. 2nd Edition. Wiley-Interscience publication. 1981. Print.

Bloomberg, Dan. *Rotation*. <http://www.leptonica.com/rotation.html>, April 20th, 2016

Bugayevskiy, Lev, and Snyder, John. *Map Projections: A Reference Manual*. Taylor & Francis, 1995. Print.

CCD 442A 2048x2048 Element Full Frame Image Sensor. Fairchild Imaging. Date unknown.

EPIC Instrument Description Document. Document 2E19316-NC. 11 October, 2001

EPIC User's Guide. Document DSCOV-EPIC-OPS-xxxx. 2011



Hohenkerk, C.Y., Sinclair, A.T. *The Computation of Angular Atmospheric Refraction at Large Zenith Angles*. HM Nautical Almanac Office NAO Technical Note No. 63, 1985 April. <http://astro.ukho.gov.uk/data/tn/naotn63.pdf>

Hoisington, Charles. *How We Did It*. May, 2001

Iliffe, Jonathan, and Lott, Rodger. *Datums and Map Projections for Remote Sensing, GIS and Surveying*. 2nd Edition. Whittles Publishing, 2008. Print.

Gonzalez, Rafael, and Woods, Richard. *Digital Image Processing*. 2nd Edition. Prentice Hall, 2001.

Meeus, Jean. *Astronomical Algorithms*. 2nd Edition. William-Bell, Inc. 2009. Print.

Meeus, Jean. *Astronomical Formulae for Calculators*. 4th Edition. William-Bell, Inc, 1988. Print.

Schreirer, R, Dybbrore, A., Raspaud, M. *A General Approach to Enhance Short Wave Satellite Imagery by Removing Background Atmospheric Effects*. Remote Sensing, April 5th 2018

Stevens' Power Law. https://en.wikipedia.org/wiki/Stevens'_power_law April 25, 2016

Triana Attitude and Orbit Control System Hardware Coordinate System Document. Document TRIANA-SPEC-052 Revision B. July 27, 2000

Wertz, James. *Spacecraft Attitude Determination and Control*. Reidel Publishing Company, 1978. Print.

Westland, S., Ripamonti, C., and Cheung, V. *Computational Colour Science Using Matlab*. 2nd Edition. Wiley, 2012. Ebook.

Wyckoff, C.W. and McCue J.C. *A Study to Determine the Optimum Design of a Photographic Film for the Lunar Surface Hand-Held Camera*. NASA CR92015, 1965. Print.

Wyszecki, G and Stiles, W. *Color Science: Concepts and Methods, Quantitative Data and Formulae*. 2nd Edition. Wiley Classics Library, 1982. Print.

Yang, Kai, et al. "MODIS band-to-band registration." *Geoscience and Remote Sensing Symposium, 2000. Proceedings. IGARSS 2000. IEEE 2000 International*. Vol. 2. IEEE, 2000.

